## Case Report
# Breast implant-associated ALK-negative anaplastic large cell lymphoma: a case report and discussion of possible pathogenesis

Eva V George[1], John Pharm[2], Courtney Houston[3], Semar Al-Quran[1], Grey Brian[1], Huijia Dong[1], Wang Hai[1], Westley Reeves[4], Li-Jun Yang[1]

[1]Departments of Pathology, Immunology, Laboratory Medicine, [4]Medicine, University of Florida College of Medicine, Gainesville, FL 32607; Departments of [2]Pathology and [3]Surgery, John D Archbold Memorial Hospital, Thomasville, GA 31799, USA

**Abstract:** Breast implant associated anaplastic large cell lymphoma (BIA-ALCL) is a recently recognized clinical entity, with only 39 well-documented cases reported worldwide, including 3 fatalities. Because of its rarity, the clinical and pathologic features of this malignancy have yet to be fully defined. Moreover, the pathogenesis of ALCL in association with textured silicone gel breast implants is poorly understood. Here we report a case of BIA-ALCL arising in a 67-year-old woman with a mastectomy due to breast cancer followed by implantation of textured silicone gel breast prosthesis. The patient presented with breast enlargement and tenderness 8 years following reconstructive surgery. MRI revealed a fluid collection surrounding the affected breast implant. Pathologic examination confirmed the presence of malignant ALCL T cells that were CD30+, CD8+, CD15+, HLA-DR+, CD25+ ALK- and p53. A diagnosis of indolent BIA-ALCL was made since tumor cells were not found outside of the capsule. Interestingly, an extensive mixed lymphocytic infiltrate and ectopic lymphoid tissue (lymphoid neogenesis) adjacent to the fibrous implant capsule were present. The patient was treated with capsulectomy and implantation of new breast prostheses. Six months later, the patient was found to have BIA-ALCL involvement of an axillary lymph node with cytogenetic evolution of the tumor. To our knowledge, this is the sixth reported case of aggressive BIA-ALCL. Unique features of this case include the association with lymphoid neogenesis and the in vivo cytogenetic progression of the tumor. This case provides insight into the potential role of chronic inflammation and genetic instability in the pathogenesis of BIA-ALCL.

**Keywords:** Anaplastic large cell lymphoma (ALCL), breast implant, ectopic lymphoid aggregates, pathogenesis, ALK-negative

## Introduction

It has long been speculated that breast implants may increase the risk of developing systemic connective tissue disease and malignancy [1-3]. However, until recently, epidemiological evidence was lacking. In 2011, the US Food and Drug Administration published a report [4] supporting an association between textured silicone or saline breast implants and the development of anaplastic lymphoma kinase (ALK) negative anaplastic large T cell lymphoma (ALCL), a rare form of Non-Hodgkin's lymphoma [5]. This is a new clinical entity, with 39 well-documented cases reported worldwide [6], including 3 fatalities [6-9]. Nearly all of these neoplasms have developed in association with textured silicone breast implants [4, 9-24]. However, the pathological and clinical features of breast implant-associated (BIA)-ALCL remain to be fully defined. It is critical to document all cases of BIA-ALCL in order to further define its epidemiology, pathologic features, clinical behavior, classification, prognosis, and pathogenesis.

Most BIA-ALCL occur in association with cosmetic breast implants [25-27], supporting a causal role for the breast implant itself. Whereas the vast majority of primary breast lymphomas (95%) are of B-cell origin [28], BIA-ALCL are predominantly T-cell neoplasms [3],

with only 3 cases of B-cell lymphomas described in association with breast implants [7]. ALCL, a rare form of T-cell non-Hodgkin's lymphoma (NHL), is classified as systemic, secondary, or primary cutaneous [28]. Systemic ALCL often follow an aggressive clinical course and is usually driven by ALK expression. BIA-ALCL has been suggested to more closely resemble primary cutaneous ALCL [6], which is frequently ALK-negative and follows an indolent course. However, BIA-ALCL has many unique clinical and pathological features, suggesting that it is a separate disease entity.

The recognition of BIA-ALCL as a new clinical entity raises many questions. What are the defining clinical, pathological, and molecular features of this malignancy? Why and how do textured breast implants trigger malignant transformation in some patients but not in others? What are the pathogenic mechanisms? What distinguishes indolent tumors from aggressive ones? The answers to these questions will require close study of additional patients. Here, we report a unique case of BIA-ALCL in a 68 year-old woman that initially presented as an indolent clonal tumor restricted to the seroma and capsule surrounding the implant that then, over 6 months, evolved into a more aggressive tumor involving local lymph nodes and displaying additional chromosomal abnormalities arising through in vivo clonal evolution. We discuss features of this tumor and associated ectopic lymphoid tissue surrounding the capsule of the implant that may be relevant to the pathogenesis and evolution of BIA-ALCL tumors.

**Case history**

A 67-year old white woman with ductal carcinoma in situ of the right breast underwent simple mastectomy in 2001. This was followed by reconstruction with tissue expander (Style 133 LV 400 ml Allergan tissue expander), which was later replaced with a style 153 m 540 ml textured double-lumen silicone gel implant. In 2004 she was diagnosed with comedo carcinoma in situ in the left breast, for which she underwent simple left mastectomy followed with the same style tissue expander for reconstruction and a style 153, 360 mL Allergan double-lumen silicone-gel textured implant (LOT-3344454-MCGHAN-360CC). At that time, her right breast implant was replaced with the

same type of double-lumen silicone-gel textured implant (LOT-273111-MCGHAN-360CC). Her course was unremarkable until 2012, when she presented with a 4-5 month history of enlargement and tenderness of the right breast. She had fallen recently and it was initially thought that she might have injured her breast. On exam, the right breast was 2-3 times the size of the left, tense and very tender. Her left breast was unremarkable. The differential diagnosis included hematoma, seroma, and ALCL. A bilateral breast MRI with and without contrast revealed a large fluid collection surrounding the right breast implant (**Figure 1**) and a radial fold within the implant. In the posterior aspect of the inner shell of the right breast implant there was a silicone signal extending into the outer shell, consistent with intracapsular gel bleed or, possibly, intracapsular rupture into the outer capsule. The right breast contained a large collection of straw-colored fluid that was sent for cytology, histology, flow cytometry, and culture. A portion of the thick fibrous capsule was sent for histology. Cultures were negative, but pathology of both the proteinaceous material in the fluid and the fibrous capsule revealed involvement by ALCL (see results). The patient did not receive chemotherapy or radiation therapy after undergoing bilateral capsulectomy and implant replacement.

A follow up PET scan revealed a small focus of mildly increased radiotracer activity corresponding to a minimally prominent precarinal lymph node. This was felt most likely to represent reactive lymphadenopathy, though metastatic disease could not be excluded. Six months later, a repeat PET scan showed radiotracer activity in the internal mammary chain, precarinal, and right axillary lymph nodes. Based on these changes, a partial right axillary lymph node dissection was performed and one of three lymph nodes examined was found to contain tumor cells.

**Materials and methods**

*Cytology and pathology*

A portion of the fibrous capsule surrounding the breast implant and subsequent lymph node biopsy were sent for pathological examination. For histopathology, the capsule and surrounding breast tissue and lymph nodes were embedded in paraffin and sections were stained with
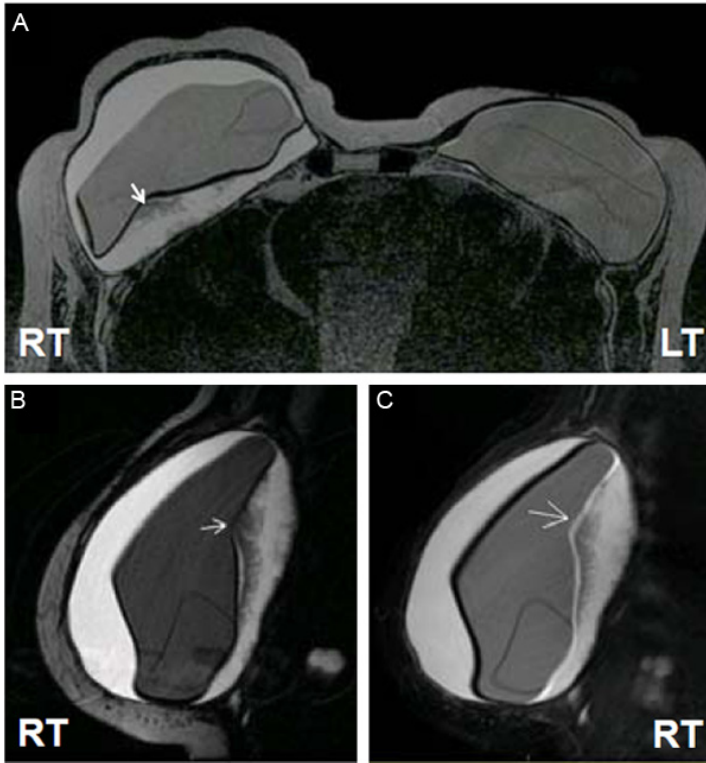
**Figure 1.** Breast MRI. Bilateral breast MRI (A) reveals a fluid collection surrounding the right breast implant as well as a radial fold within the right breast implant (arrow). There is a silicone signal extending from the posterior aspect of the inner shell to the outer aspect of the implant (B and C), suggesting an intracapsular gel bleed or possibly intracapsular rupture.

finization and antigen epitope retrieval, two different primary antibodies were applied sequentially to the tissue. The first target antigen was visualized by the Ultra View DAB detection kit (dark-brown color). The antibodies were removed by heating, whereas the brown stain remained. The slides then were incubated with the second primary antibody and target antigen was visualized by the Ultra View Alkaline Phosphatase Red detection kit to highlight the second antigen in red color.

*Flow cytometry*

Single cell suspensions were stained with fluorescently-conjugated antibodies (CD30, HLA-DR, CD45, CD25, CD3, CD4, CD5, CD8, CD5, CD20 and CD19). All antibodies and isotype controls were purchased from BD Biosciences (San Jose, CA). Samples were analyzed on a FACS Calibur flow cytometer (BD Biosciences) and data (10,000 events per sample) were analyzed using FCS express 4 plus software.

hematoxylin and eosin (H&E). Fluid from the implant capsule was sent for cytological examination and flow cytometry. Cytospin slides were stained with Wright-Giemsa and cell blocks were prepared by standard protocols for H&E sections and immunostaining.

*Immunohistochemtry (IHC) and double-IHC*

Four μM paraffin sections were placed on plus slides and dried for 2 hours at 60°C. The slides were subjected to dewaxing and antigen retrieval with Ventana's CC1 retrieval solution for 30 min at 95-100°C on a Ventana Benchmark automated stainer. Dako prediluted primary antibodies (CD30, CD15, CD3, CD20, CD4, CD8, ALK-1, p53, and Ki67) were applied to sections at 37°C for 32 minutes. Antigen was visualized by using the Ultra View DAB kit (Ventana Medical Systems Inc. Tucson AZ). Slides were counterstained with Ventana hematoxylin and then dehydrated, cleared, and mounted. For double IHC, following de-paraf-

*Analysis of TCR γ-chain gene rearrangements*

TCR γ-chain rearrangement was analyzed by polymerase chain reaction (PCR) according to published procedures [29] using extracted DNA from cells isolated from the peri-implant fluid. Multiplex PCR was performed using nested primers encompassing the V and J regions. PCR products were separated on a 2.75% Metaphor agarose gel and imaged by AlphaImager HP system (Cell Bioscience, INC, Santa Clara, California).

*Conventional cytogenetic studies*

Cells isolated from the peri-implant fluid and lymph nodes were cultured for 24 or 48 hours in RPMI-1640 medium containing 20% fetal bovine serum prior to harvesting mitotic cells following standard cytogenetic techniques. Chromosome spreads were G-banded by the standard Trypsin-Giemsa banding (GTG) technique. Twenty metaphase cells were analyzed
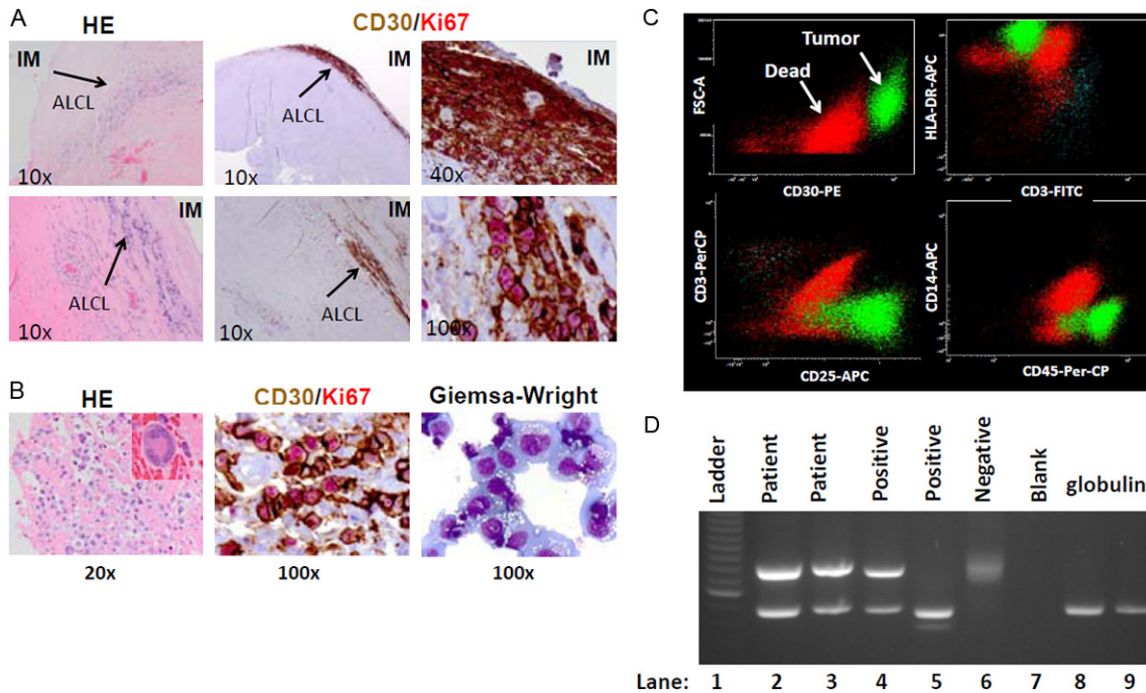
**Figure 2.** Diagnosis of characterization of BIA-ALCL. A. H&E section of the right breast capsule reveals tumor cells infiltrating along the edge of the capsule (arrows). Double IHC with CD30/Ki67 highlights tumor cells uniformly positive for CD30 and Ki67 (greater than 90%). B. H&E section of the cell block (left), CD30/Ki-67 IHC (middle) and Giemsa-Wright stained cytospin (right panel) of tumor cells show abundant and vacuolated cytoplasm typical cytologic features of ALCL cells. A large, pleiomorphic tumor cell with horseshoe-shaped nuclei (insert) is shown at higher magnification. C. Flow cytometric analysis of tumor cells confirms strong staining for CD30, CD45, HLA-DR and CD25. D. PCR analysis confirms clonal T-Cell Receptor (TCR) γ gene rearrangement in tumor cells, as indicated by the distinct bands (in contrast to the negative control demonstrating a smear).

by bright-field oil immersion microscopy using computer-assisted imaging and karyotyping software.

## Results

This patient presented with a 4-5 month history of enlargement and tenderness of the right breast 8 years following breast reconstruction with a textured silicone implant. Pathological examination of the serous fluid surrounding the implant and the fibrous capsule confirmed a diagnosis of BIA-ALCL. The patient was treated with capsulectomy and replacement of the implants without chemotherapy. A PET scan 6 months later revealed possible lymph node involvement by BIA-ALCL, which was confirmed with node biopsy.

*Pathologic findings at time of diagnosis*

H&E sections revealed dense fibrosis and large atypical cells closely adjacent to the surface of the right implant capsule (**Figure 2A**). CD30

and Ki67 IHC revealed that the atypical large cells were positive for CD30 and Ki-67 (>90%), indicating a high proliferative index. The tumor cells were also positive for CD15, CD8, perforin and negative for ALK1 (data not shown), an immunophenotype consistent with ALK-negative ALCL. **Figure 2B** revealed that ALCL cells from the seroma fluid were large and pleiomorphic (insert), often with horseshoe-shaped nuclei and vacuolated abundant cytoplasm, a cytologic feature of highly proliferative cells (CD30+/Ki-67+) and extensive tumor cell necrosis.

Flow cytometry of the tumor cells confirmed strong staining for CD45, CD30, HLA-DR, CD25, and negative staining for CD3. PCR performed on DNA extracted from the tumor cells in the serous fluid demonstrated a clonally rearranged TCR γ-chain (**Figure 2C**) with no evidence of clonal B-cell immunoglobulin heavy (IgH) chain gene rearrangement (data not shown), confirming the tumor cells' T-cell origin and clonal derivation.
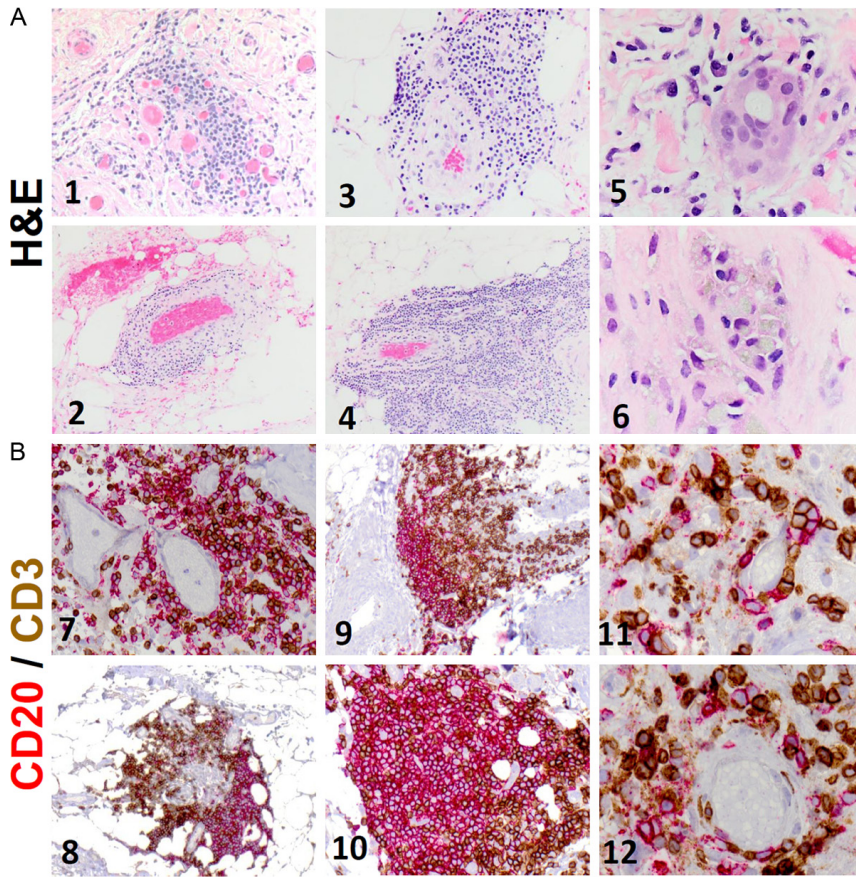
**Figure 3.** Inflammatory cells and ectopic lymphoid tissue within capsule. A. H&E staining of sections of the breast-implant capsule shows a robust infiltrate of lymphocytes, monocytes, plasma cells (1-4), giant cells (5) and foamy macrophages (6) engulfing amorphous material, which is likely to be silicone. B. Immunohistochemical staining of sections of the breast-implant capsule with CD3 and CD20 demonstrates that the lymphocytic infiltrate is composed of both B-cells (red) and T-cells (brown). Distinct T-cell and B-cell zones can be seen (8-10), reminiscent of ectopic lymphoid tissue. The T-cells appear to exhibit more infiltrative behavior, extending deeper into the capsule (9). B- and T-cells can be seen aggregating adjacent to blood vessels (11-12).
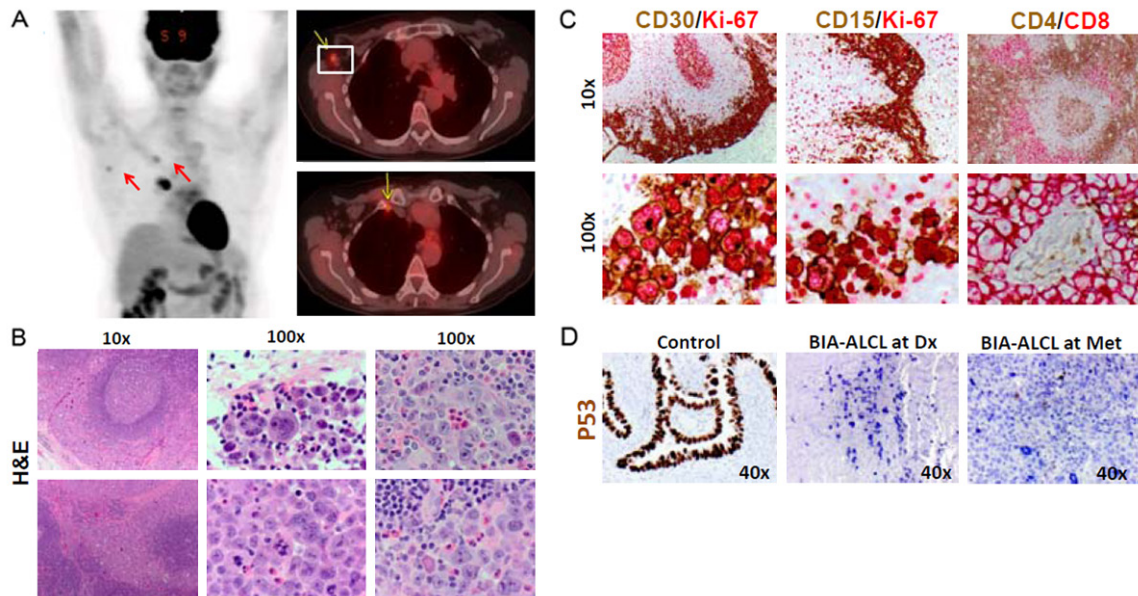


**Figure 4.** PET scan and biopsied lymph node (six month later). A. A follow-up PET scan 6-months after diagnosis showed hyperintense signals in mediastinal, para-aortic, and axillary lymph nodes. B. Lymph node biopsy confirmed involvement by ALCL. Low magnification shows tumor cells invading in a sinusoidal cohesive pattern. Higher magnification shows the severe nuclear atypia, pleomorphism of tumor cells, as well as marked increased eosinophils. C. Immunohistochemical staining of lymph node confirmed BIA-ALCL with expression of CD30, CD15, CD8 and high proliferative index for Ki67. D. Immunohistochemical staining of lymph node with p53 antibodies revealed no expression of p53 at diagnosis (middle) or relapse or metastasis (right panel).
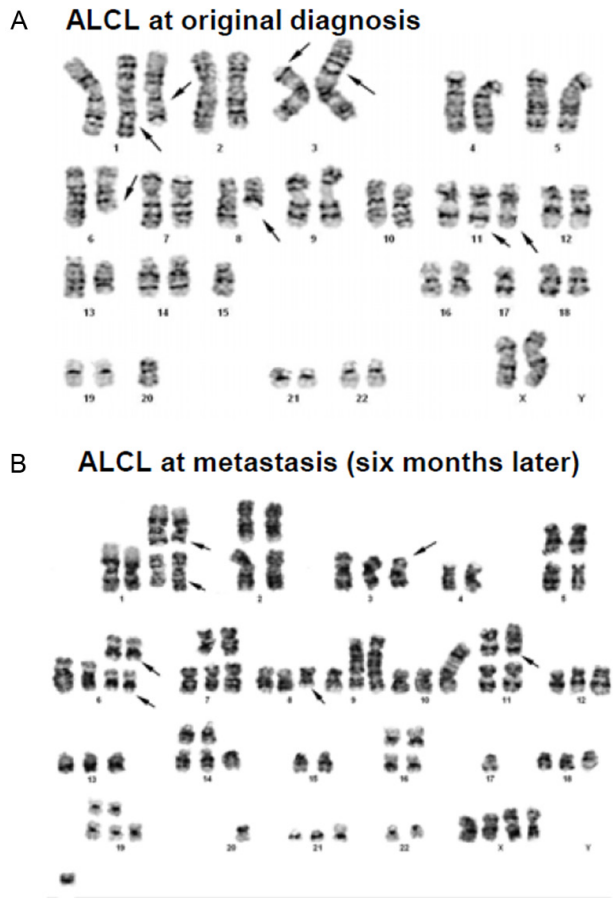
**Figure 5.** Karyotypic analysis shows tumor cell clonal evolution. A. Karyotypic analysis of tumor cells at diagnosis shows a highly complex karyotype, with numerous chromosomal abnormalities. The multiple clonal cytogenetic abnormalities are listed in Table 1. B. Karyotypic analysis of tumor cells at the time of relapse shows a much more complex karyotype than the primary tumor cells. Arrows marked the shared chromosomal abnormalities as germlines. The multiple clonal cytogenetic abnormalities are listed in Table 1 for comparison.

*Ectopic lymphoid tissue formation (lymphoid neogenesis)*

The capsule surrounding the patient's textured silicone breast implant exhibited a robust mixed inflammatory infiltrate surrounding the T cell tumor. H&E staining showed abundant lymphocytes, monocytes, and plasma cells, along with scattered giant cells and foamy macrophages engulfing amorphous material, likely silicone gel (**Figure 3A**). Co-immunohistochemical staining with CD3 and CD20 antibodies revealed that the lymphocytic infiltrate was comprised of both B- and T-cells (**Figure 3B**). In some fields, these were organized into distinct T-cell and B-cell zones, consistent with the formation of ectopic lymphoid tissue. Interestingly, the

T-cells appeared to follow a more infiltrative pattern, reaching deeper into the breast implant capsule, suggesting that these may be the cells the directly interact with the foreign implant material possibly priming them for malignant transformation.

*Radiologic and pathologic findings at relapse*

Follow-up PET imaging revealed hyperintense foci in three lymph nodes, one mediastinal, one para-aortic, and one axillary (**Figure 4A**), suspicious for possible lymph node involvement by ALCL. Random biopsy of the nodes revealed partial involvement by ALCL. The tumor cells infiltrated the lymphoid tissue in a sinusoidal cohesive pattern and were highly pleomorphic, with greater nuclear atypia than was observed in the primary tumor (**Figure 4B**). Many multinucleated giant cells with abundant cytoplasm and prominent nucleoli along with frequent mitotic figures were present in a background of small lymphocytes and numerous eosinophils, consistent with aggressive tumor behavior.

As expected, IHC staining for CD30 and Ki67 revealed intense and diffuse positivity (**Figure 4C**). Interestingly, the CD15+ tumor cell population was increased in the relapsed tumor, suggesting that CD15 may mark a more aggressive subclone arising from the original ALCL. CD4 and CD8 co-staining showed cohesive CD8+ tumor cell clusters embracing lymphoid follicles and surrounding blood vessels in a background of CD4+ reactive T cells. In addition to confirming the tumor cell phenotype, the immunostaining also highlighted sinusoidal and paravesicular tumor cell infiltration, consistent with the pathological features of ALCL. IHC staining with anti-p53 antibodies showed the absence of p53 protein expression in tumor cells at diagnosis and rare expression in metastatic tumor cells (**Figure 5C**), suggesting that some defects in p53 pathway might contribute to tumorigenesis and genetic instability.

*Karyotypic analysis*

Karyotypic analysis of tumor cells at initial diagnosis demonstrated multiple chromosomal abnormalities (**Figure 5A**, **Table 1**). An abnor-

mal near-diploid cell population bearing a highly complex karyotype with multiple numerical and structural clonal cytogenetic aberrations and a near-tetraploid version of this abnormal population were identified in metaphase cells examined from a stimulated culture of cells harvested from the fluid sample. It is worth noting that the absence of a normal copy of chromosome 17 in this karyotype may reflect a loss of heterozygosity of the TP53 (tumor suppressor) gene locus, which generally is considered to represent an unfavorable indicator of an advancing or evolving tumor cell population. Interphase FISH analysis revealed no evidence of ALK gene rearrangement except for an ALK copy number change due to ploidy change.

At the time of relapse, tumor cells were again subjected to karyotypic analysis, which demonstrated even more complex numerical and structural chromosomal abnormalities (**Figure 5B**, **Table 1**). Comparison between the original and relapsed clonal tumor cell signatures of the shared chromosomal abnormalities and ploidy changes, strongly suggests that the relapsed tumor clones are derived from the original tumor clones, as evidenced by the shared stemline structural cytogenetic aberrancies highlighted in bold (**Table 1**) and by arrows in **Figure 5**. The observation that the relapsed tumor cells possess multiple new cytogenetic abnormalities suggests that in vivo tumor cell genetic evolution and selection due to marked intrinsic genetic instability may contribute to tumor progression and acquisition of an aggressive phenotype in BIA-ALCL.

**Discussion**

BIA-ALCL is a newly defined clinical entity that may present as early as 1 year after breast augmentation/reconstruction or as late as 32 years afterward (mean 10.5 years) [6]. As illustrated by the present case, the tumor presents as a recurrent or unremitting seroma and/or tumor mass attached to a scar capsule containing malignant T-cells [30]. Although BIA-ALCL has been suggested to follow an indolent clinical course, aggressive and fatal cases have been reported. The actual incidence of aggressive BIA-ALCL cannot yet be accurately determined as long-term follow-up is lacking. The case we report here is unique in that it was first recognized as an indolent tumor, which then underwent transformation to an aggressive

ALCL with evidence of *in vivo* cytogenetic evolution six months post-capsulectomy without chemotherapy. Consistent with previous reports [4, 9-24], the tumor cells were highly proliferative, formed cohesive sheets of pleomorphic, epithelioid-like cells infiltrating tissues and lymph nodes, strongly expressed CD30, demonstrated clonally rearranged TCR genes, were ALK-, and exhibited complex cytogenetic abnormalities. The complexity of these cytogenetic abnormalities and their evolution with tumor progression suggests that genetic instability may be central to BIA-ALCL pathogenesis, perhaps in a susceptible patient population.

*Indolent versus aggressive ALCL*

BIA-ALCL is generally an indolent disease localized to the breast implant and effectively treated with capsulectomy alone without chemotherapy. However, the limited long-term follow-up in many previous reports makes it difficult to accurately assess the frequency of disease relapse and/or progression. A small subset of cases has been reported to be aggressive (**Table 2**), demonstrating extra-capsular involvement and requiring extensive therapy [7, 8, 16, 25, 30] with three well-documented fatal cases [6-8]. The patient reported here represents another aggressive case of BIA-ALCL, presenting with lymph node involvement six months after capsulectomy. She received the chemotherapy regimen (CHOP + Etoposide) after the lymph nodes were found to be positive (for 4 cycles) and a repeat PET scan is negative. This suggests that BIA-ALCL should not be assumed to be indolent, and that a thorough workup at diagnosis may be indicated along with long-term routine follow up.

The aggressive clinical course of some BIA-ALCLs may be due to intrinsic behavior of the initial tumor clone or may represent an advanced stage of disease at diagnosis with already established micrometastases. If intrinsic aggressive behavior is responsible, it is possible that two different forms of BIA-ALCL coexist, one indolent and the other aggressive. The aggressive form may arise by different mechanisms. Although the sample size to-date is very small, the aggressive tumors reported previously, like the one here, have arisen in patients with breast implants secondary to reconstructive surgery following breast cancer, suggesting

**Table 1.** Tumor cells in vivo cytogenetic evolution

| Cell Source | Timeline | Clonal Cytogenetic Abnormalities | Interpretation |
|---|---|---|---|
| Tumor cells from seroma fluid | Original Tumor clones 4/18/12 | **45, XX [cp19]**<br>**dup(X)(q11q28), +1, del(1)(q32), i(1)(q10), add(3)(p11), der(3) t(2;3)(p12;p26), +6, der(6)t(6;8)(q12;q21.3)x2, add(8)(q11.2), add(11)(q23), add(14)(p11.1), -15, -17, -20**<br>**80~91, idem [cp2]** | An abnormal near-diploidy cell population (19/21) bearing a highly complex karyotype and a near-tetraploidy version (2/21) were detected in metaphase cells by conventional G-banding techniques. The 97.7% of this abnormal population showed negative ALK rearrangement with an ALK copy number change by interphase FISH techniques. |
| Cells from lymph node | Secondary Tumor Clones 10/19/12 | 34, XX [1]*<br>**+1**, del(1)(q32)x2, +2, -3, **der(3)t(2;3)(p12;p26)**, **+6**, **der(6)t(6;8) (q12;q21.3)x2**, add(9)(p22), -10, -12, -12, -13, -14, **-15**, add(15) (p11.2), -16, add(16)(q11.2), **-17**, -18, **-20, -20**, -21, -21, -22 [1]<br>78-79, XX [cp3]*<br>+X, +X, **+1, +1, del(1)(q32)x2, i(1)(q10), +2, add(3)(p11)**, add(4) (q21), +6, +6 **der(6)t(6;8)(q12;q21.3)x2**, -8, add(9)(p22)x1-3, -10, add(10)(p13), **add(11)(q23)**, +14, **-15**, add(15)(p11.2), +16, add(16)(q11.2)x2, **-17**, -17, -18, +19, **-20**, -22, i(22)(q10), +mar1-2<br>46, XX [16] | Two related (variant) abnormal cell populations bearing highly complex karyotypes were detected in 4/20 metaphase cells. Of the four, one is a hyperhaploidy with chromosome count of 34, while the remaining three contained a hypertriploidy with chromosome count of 78-79. Common clonal cytogenetic changes observed among these abnormal cells indicate ploidy variants (or evolution) of a stemline or primary cell population. |

*Bold-highlighted cytogenetic abnormalities are shared by original and secondary tumor clones.

**Table 2.** Aggressive cases of BIA-ALCL

| Case/Ref. | Age/Int. at ALCL, PMH | Textured BI filled with | Presentation/ Sites of disease | Markers | Genetics/ ALK Status | Treatment/ Outcome |
|---|---|---|---|---|---|---|
| Alobeid et al. 2009 | 68/16, history of Rt breast ductal CA and PBC | silicone | Rt axillary LAD/Rt axillary LNs, Rt BI capsule, Lt axillary LNs | CD30+, CD45-/+, CD15+, CD2+, CD4+, EMA+, MUM1+ | complex ALK- | CPT, 6 cycles CHOP/No known relapse |
| Carty et al. 2011 | 57/32, multiple BI revisions due to capsular contraction and implant rupture | silicone | B-symptoms, Lt axillary LAD/Lt BI capsule with chest wall invasion and pleural thickening | CD30+, CD4+ | Complex ALK- | CPT, RT, 5 cycles CHOP, salvage CT, ASCT/Death from progressive disease 3 years after diagnosis |
| Gaudet et al. 2002 | 50/10, Lt breast CA, remote history of HL | Silicone | Mass overlying Rt BI/Dermal involvement overlying Rt BI | CD30+, CD2+, LCA+, weakly positive for CD3, CD5, CD43 | Complex ALK- | CHOP/Relapse 1 year later with pleural and pericardial effusions, mediastinal LAD; Unknown current status |
| Aladily et al. 2012 | 63/6+1, L breast CA, 3 yr history of lyP | saline | Effusion & mass in Rt breast/Rt breast | CD30+, CD3+, CD4+, CD2+, CD43+ | Complex ALK- | CPT/Died at 12 yrs post ALCL diagnosis |
| Aladily et al. | 47/9, breast CA | saline | Rt BI mass/Rt breast with effusion | CD30+, CD45+, CD43+, CD4+, EMA+, Granzyme B | Complex ALK1- | CPT, RT, CT/Died at 2 yrs post ALCL diagnosis |
| Our Case | 67/8, breast CA | Silicone | Enlargement and Effusion in Rt breast/Rt breast | CD30+, CD15+, CD25+, CD8+, | Complex with genetic evolution ALK- | CPT at diagnosis, CHOP/ Etoposide at relapse. Patient is well without detectable disease |

Int., interval; Rt, right; Lt, left; BI, breast implant; CA, carcinoma; LN, lymph node; LAD, lymphadenopathy; LyP, lymphomatoid papulosis; CPT, capsulectomy; RT, radiation therapy; CT, chemotherapy; ASCT, autologous stem cell transplantation; CHOP, PBC, primary billiary cirrhosis; ALK-, anaplastic lymphoma kinase gene rearrangement negative; Ref., reference.

that these patients may be predisposed to malignancy. Indeed, the patient reported here developed cancer in both breasts. This raises the possibility that this group of patients has an inherent genetic instability, which is exaggerated when put under pressures such as a robust inflammatory response that enhance the need to protect genome integrity.

Conversely, if advanced, metastatic disease is present but undetected at diagnosis, a more thorough workup at the time of diagnosis and closer follow-up of the patients might be indicated to determine the full extent of disease. Furthermore, recognizing that micrometastatic disease may be present at diagnosis suggests that the therapeutic approach may need revision as well. Perhaps capsulectomy is not a sufficiently aggressive treatment for BIA-ALCL, as it would not eliminate micrometastases.

*Genetic instability and BIA-ALCL*

An interesting and consistent feature of BIA-ALCLs is their complex cytogenetics. This suggests that genomic instability may play a role in tumorigenesis and/or tumor progression. Indeed, the absence of a normal copy of chromosome 17 in the current case reflects a loss of heterozygosity of the TP53 (tumor suppressor) gene locus located on the short arm of chromosome 17 (17p13.1), which may have contributed to the aggressiveness of this patient's tumor. Since the p53 antibodies used for IHC recognize both normal and mutant p53, the tumor cells may either be p53 null or defects in p53 pathway when the tumor cells exhibited such abnormal ploidy and mitosis [31]. Human p53 plays an important role in apoptosis, genomic stability, and inhibition of angiogenesis [32]. It is possible that slight defects in the maintenance of genetic integrity are only uncovered when these mechanisms to go into overdrive, such as during a robust inflammatory response [33], and hypoxia as seen in some patients with textured breast implants.

Consistent with that model, this patient's tumor exhibited increasingly complex karyotypic changes as the tumor evolved from an apparently indolent neoplasm to an invasive lymphoma extending beyond the breast implant capsule and into lymph nodes. It is plausible that specific chromosomal changes act as 'driver'

mutations responsible for tumor aggressiveness and identifying these will be critical to developing rationally designed therapeutic strategies. In addition to p53, genes involved in maintaining genetic integrity in immune cells, such as activation-induced cytidine deaminase (AID) are implicated in the pathogenesis of other inflammation-related neoplasms [34, 35], and also could be involved BIA-ALCL. Indeed, transgenic mice with constitutive AID expression [36] and p53 deficiency [37] develop T-cell lymphoma.

*Breast implants, inflammation, and ALCL*

Inflammation has been linked to tumorigenesis and tumor progression in many malignancies [34, 38, 39]. The strong association between texturized breast implants and ALCL development suggests that the foreign biomaterial may instigate neoplastic transformation, probably by triggering a chronic inflammatory response. The ectopic lymphoid tissue surrounding the T cell neoplasm in the present case provides compelling evidence in support of this hypothesis. The formation of ectopic lymphoid tissue ("lymphoid neogenesis") is a frequent manifestation of chronic inflammation [40, 41]. Lymphoid neogenesis is associated with chronic inflammation in infections such as chronic hepatitis C and *Helicobacter pylori* infection [34, 42] and chronic autoimmune diseases such as autoimmune thyroiditis, Sjogren's syndrome, rheumatoid arthritis, primary biliary cirrhosis, and lupus [40, 43]. Interestingly, all of these chronic inflammatory conditions are associated with the development of lymphomas, which typically arise extranodally within the chronically inflamed tissues. Although T cell lymphomas have been reported, B cell lymphomas are far more common [17]. The lymphoid neogenesis seen in BIA-ALCL is unusual in that it appears to promote the development of T cell, rather than B cell, neoplasia. This could reflect the type of inflamed tissue, subcutaneous tissue or perhaps breast tissue, instead of glandular tissue (thyroid, salivary glands), solid organs (liver), or joints. Alternatively, it could be a consequence of the material inciting the inflammatory response, in this case textured silicone elastomer. The occurrence of cutaneous ALCL following insect bites [44] lends some support to the former hypothesis. A murine model of autoimmune disease associated with chronic inflammation (lymphoid neogenesis),

pristane-induced lupus, is associated with B cell neoplasia [45, 46]. Unfortunately, a comparable mouse model for BIA-ALCL does not yet exist. If such a model could be established, it may be invaluable in resolving the issue of why textured silicone breast implants predispose to T cell lymphoma genesis.

## Acknowledgement

Address correspondence to: Dr. Li-Jun Yang, Department of Pathology, Immunology, Laboratory Medicine, Dental Science Building Rm D6-28, University of Florida, Gainesville, FL 32607. Phone: 352-392-0005; E-mail: yanglj@pathology.ufl.edu

## References

[1] Brinton LA and Brown SL. Breast implants and cancer. J Natl Cancer Inst 1997; 89: 1341-1349.

[2] de JD, Vasmel WL, de Boer JP, Verhave G, Barbe E, Casparie MK and van Leeuwen FE. Anaplastic large-cell lymphoma in women with breast implants. JAMA 2008; 300: 2030-2035.

[3] Lazzeri D, Agostini T, Bocci G, Giannotti G, Fanelli G, Naccarato AG, Danesi R, Tuccori M, Pantaloni M and D'Aniello C. ALK-1-negative anaplastic large cell lymphoma associated with breast implants: a new clinical entity. Clin Breast Cancer 2011; 11: 283-296.

[4] Anaplastic Large Cell Lymphoma (ALCL) In Women with Breast Implants: Preliminary FDA Findings and Analyses. 2011.

[5] Ferreri AJ, Govi S, Pileri SA and Savage KJ. Anaplastic large cell lymphoma, ALK-negative. Crit Rev Oncol Hematol 2013; 85: 206-215.

[6] Story SK, Schowalter MK and Geskin LJ. Breast Implant-Associated ALCL: A Unique Entity in the Spectrum of CD30+ Lymphoproliferative Disorders. Oncologist 2013; 18: 301-7.

[7] Carty MJ, Pribaz JJ, Antin JH, Volpicelli ER, Toomey CE, Farkash EA and Hochberg EP. A patient death attributable to implant-related primary anaplastic large cell lymphoma of the breast. Plast Reconstr Surg 2011; 128: 112e-118e.

[8] Aladily TN, Medeiros LJ, Amin MB, Haideri N, Ye D, Azevedo SJ, Jorgensen JL, de Peralta-Venturina M, Mustafa EB, Young KH, You MJ, Fayad LE, Blenc AM and Miranda RN. Anaplastic Large Cell Lymphoma Associated With Breast Implants: A Report of 13 Cases. Am J Surg Pathol 2012; 36: 1000-1008.

[9] Aladily TN, Medeiros LJ, Amin MB, Haideri N, Ye D, Azevedo SJ, Jorgensen JL, de Peralta-Venturina M, Mustafa EB, Young KH, You MJ, Fayad LE, Blenc AM and Miranda RN. Anaplastic Large Cell Lymphoma Associated With Breast Implants: A Report of 13 Cases. Am J Surg Pathol 2012; 36: 1000-1008.

[10] Newman MK, Zemmel NJ, Bandak AZ and Kaplan BJ. Primary breast lymphoma in a patient with silicone breast implants: a case report and review of the literature. J Plast Reconstr Aesthet Surg 2008; 61: 822-825.

[11] Taylor CR, Siddiqi IN and Brody GS. Anaplastic large cell lymphoma occurring in association with breast implants: review of pathologic and immunohistochemical features in 103 cases. Appl Immunohistochem Mol Morphol 2013; 21: 13-20.

[12] Bishara MR, Ross C and Sur M. Primary anaplastic large cell lymphoma of the breast arising in reconstruction mammoplasty capsule of saline filled breast implant after radical mastectomy for breast cancer: an unusual case presentation. Diagn Pathol 2009; 4: 11.

[13] de JD, Vasmel WL, de Boer JP, Verhave G, Barbe E, Casparie MK and van Leeuwen FE. Anaplastic large-cell lymphoma in women with breast implants. JAMA 2008; 300: 2030-2035.

[14] Farkash EA, Ferry JA, Harris NL, Hochberg EP, Takvorian RW, Zuckerman DS and Sohani AR. Rare lymphoid malignancies of the breast: a report of two cases illustrating potential diagnostic pitfalls. J Hematop 2009; 2: 237-244.

[15] Fritzsche FR, Pahl S, Petersen I, Burkhardt M, Dankof A, Dietel M and Kristiansen G. Anaplastic large-cell non-Hodgkin's lymphoma of the breast in periprosthetic localisation 32 years after treatment for primary breast cancer--a case report. Virchows Arch 2006; 449: 561-564.

[16] Gaudet G, Friedberg JW, Weng A, Pinkus GS and Freedman AS. Breast lymphoma associated with breast implants: two case-reports and a review of the literature. Leuk Lymphoma 2002; 43: 115-119.

[17] Joks M, Mysliwiec K and Lewandowski K. Primary breast lymphoma - a review of the literature and report of three cases. Arch Med Sci 2011; 7: 27-33.

[18] Lechner MG, Lade S, Liebertz DJ, Prince HM, Brody GS, Webster HR and Epstein AL. Breast implant-associated, ALK-negative, T-cell, anaplastic, large-cell lymphoma: establishment and characterization of a model cell line (TLBR-

1) for this newly emerging clinical entity. Cancer 2011; 117: 1478-1489.

[19] Li S and Lee AK. Silicone implant and primary breast ALK1-negative anaplastic large cell lymphoma, fact or fiction? Int J Clin Exp Pathol 2009; 3: 117-127.

[20] Sahoo S, Rosen PP, Feddersen RM, Viswanatha DS, Clark DA and Chadburn A. Anaplastic large cell lymphoma arising in a silicone breast implant capsule: a case report and review of the literature. Arch Pathol Lab Med 2003; 127: e115-e118.

[21] Wong AK, Lopategui J, Clancy S, Kulber D and Bose S. Anaplastic large cell lymphoma associated with a breast implant capsule: a case report and review of the literature. Am J Surg Pathol 2008; 32: 1265-1268.

[22] Smith TJ and Ramsaroop R. Breast implant related anaplastic large cell lymphoma presenting as late onset peri-implant effusion. Breast 2012; 21: 102-104.

[23] Keech JA Jr and Creech BJ. Anaplastic T-cell lymphoma in proximity to a saline-filled breast implant. Plast Reconstr Surg 1997; 100: 554-555.

[24] Olack B, Gupta R and Brooks GS. Anaplastic large cell lymphoma arising in a saline breast implant capsule after tissue expander breast reconstruction. Ann Plast Surg 2007; 59: 56-57.

[25] Popplewell L, Thomas SH, Huang Q, Chang KL and Forman SJ. Primary anaplastic large-cell lymphoma associated with breast implants. Leuk Lymphoma 2011; 52: 1481-1487.

[26] Jewell M, Spear SL, Largent J, Oefelein MG and Adams WP Jr. Anaplastic large T-cell lymphoma and breast implants: a review of the literature. Plast Reconstr Surg 2011; 128: 651-661.

[27] Largent J, Oefelein M, Kaplan HM, Okerson T and Boyle P. Risk of lymphoma in women with breast implants: analysis of clinical studies. Eur J Cancer Prev 2012; 21: 274-280.

[28] Lechner MG, Lade S, Liebertz DJ, Prince HM, Brody GS, Webster HR and Epstein AL. Breast implant-associated, ALK-negative, T-cell, anaplastic, large-cell lymphoma: establishment and characterization of a model cell line (TLBR-1) for this newly emerging clinical entity. Cancer 2011; 117: 1478-1489.

[29] Theodorou I, Delfau-Larue MH, Bigorgne C, Lahet C, Cochet G, Bagot M, Wechsler J and Farcet JP. Cutaneous T-cell infiltrates: analysis of T-cell receptor gamma gene rearrangement by polymerase chain reaction and denaturing gradient gel electrophoresis. Blood 1995; 86: 305-310.

[30] Alobeid B, Sevilla DW, El-Tamer MB, Murty VV, Savage DG and Bhagat G. Aggressive presentation of breast implant-associated ALK-1 negative anaplastic large cell lymphoma with bilateral axillary lymph node involvement. Leuk Lymphoma 2009; 50: 831-833.

[31] Muller PA and Vousden KH. p53 mutations in cancer. Nat Cell Biol 2013; 15: 2-8.

[32] Wade M, Li YC and Wahl GM. MDM2, MDMX and p53 in oncogenesis and cancer therapy. Nat Rev Cancer 2012; 13: 83-96.

[33] Thomasova D, Mulay SR, Bruns H and Anders HJ. p53-independent roles of MDM2 in NF-kappaB signaling: implications for cancer therapy, wound healing, and autoimmune diseases. Neoplasia 2012; 14: 1097-1101.

[34] Matsumoto Y, Marusawa H, Kinoshita K, Endo Y, Kou T, Morisawa T, Azuma T, Okazaki IM, Honjo T and Chiba T. Helicobacter pylori infection triggers aberrant expression of activation-induced cytidine deaminase in gastric epithelium. Nat Med 2007; 13: 470-476.

[35] Komori J, Marusawa H, Machimoto T, Endo Y, Kinoshita K, Kou T, Haga H, Ikai I, Uemoto S and Chiba T. Activation-induced cytidine deaminase links bile duct inflammation to human cholangiocarcinoma. Hepatology 2008; 47: 888-896.

[36] Okazaki I, Yoshikawa K, Kinoshita K, Muramatsu M, Nagaoka H and Honjo T. Activation-induced cytidine deaminase links class switch recombination and somatic hypermutation. Ann N Y Acad Sci 2003; 987: 1-8.

[37] Harvey M, McArthur MJ, Montgomery CA Jr, Butel JS, Bradley A and Donehower LA. Spontaneous and carcinogen-induced tumorigenesis in p53-deficient mice. Nat Genet 1993; 5: 225-229.

[38] Rauch D, Gross S, Harding J, Niewiesk S, Lairmore M, Piwnica-Worms D and Ratner L. Imaging spontaneous tumorigenesis: inflammation precedes development of peripheral NK tumors. Blood 2009; 113: 1493-1500.

[39] Finnberg N, Klein-Szanto AJ and El-Deiry WS. TRAIL-R deficiency in mice promotes susceptibility to chronic inflammation and tumorigenesis. J Clin Invest 2008; 118: 111-123.

[40] Drayton DL, Liao S, Mounzer RH and Ruddle NH. Lymphoid organ development: from ontogeny to neogenesis. Nat Immunol 2006; 7: 344-353.

[41] Kratz A, Campos-Neto A, Hanson MS and Ruddle NH. Chronic inflammation caused by lymphotoxin is lymphoid neogenesis. J Exp Med 1996; 183: 1461-1472.

[42] Kong J, Deng X, Wang Z, Yang J, Zhang Y and Yu J. Hepatitis C virus F protein: A double-edged sword in the potential contribution of chronic inflammation to carcinogenesis. Mol Med Rep 2009; 2: 461-469.

[43] Park YW, Pryshchep S, Seyler TM, Goronzy JJ and Weyand CM. B cells as a therapeutic target in autoimmune diseases. Expert Opin Ther Targets 2005; 9: 431-445.

[44] Lamant L, Pileri S, Sabattini E, Brugieres L, Jaffe ES and Delsol G. Cutaneous presentation of ALK-positive anaplastic large cell lymphoma following insect bites: evidence for an association in five cases. Haematologica 2010; 95: 449-455.

[45] Reeves WH, Lee PY, Weinstein JS, Satoh M and Lu L. Induction of autoimmunity by pristane and other naturally occurring hydrocarbons. Trends Immunol 2009; 30: 455-464.

[46] Potter M, Morrison S and Miller F. Induction of plasmacytomas in genetically susceptible mice with silicone gels. Curr Top Microbiol Immunol 1995; 194: 83-91.